# Velocity-Shear-Driven Drift Waves with Simultaneous Azimuthal Modes in a Barium-Ion Q-machine Plasma



doi: 10.1063/1.2102747

# Velocity-shear-driven drift waves with simultaneous azimuthal modes in a barium-ion Q-machine plasma

T. Kaneko[a)]
*Department of Electronic Engineering, Tohoku University, Sendai 980-8579, Japan*

E. W. Reynolds
*Physics Department, West Virginia University, Morgantown, West Virginia 26505-6315*

R. Hatakeyama
*Department of Electronic Engineering, Tohoku University, Sendai 980-8579, Japan*

M. E. Koepke
*Physics Department, West Virginia University, Morgantown, West Virginia 26505-6315*

(Received 19 May 2005; accepted 9 September 2005; published online 19 October 2005)

Low-frequency instabilities modified by a field-aligned flow velocity shear are investigated, where the shear is controlled using a concentrically three-segmented ion emitter in a modified double-ended Q-machine [T. Kaneko *et al.*, Rev. Sci. Instrum. **73**, 4218 (2002)]. When the barium-ion flow velocity shear is produced by applying different bias voltages to two of the three segments of the ion source, drift waves having azimuthal mode number $m=1$, 2, and 3 are observed to be excited simultaneously. It is found that the excitation-threshold value of the shear strength depends on the azimuthal mode number, as expected from a model based on kinetic theory, suggesting that the observations are explained by the competition between inverse electron Landau damping and shear-modified ion Landau damping. © *2005 American Institute of Physics*.
[DOI: 10.1063/1.2102747]

## I. INTRODUCTION

Sheared ion flow parallel to magnetic-field lines has been widely investigated theoretically and experimentally, and is reported to generate various kinds of low-frequency instabilities such as D'Angelo mode,[1–8] ion-acoustic,[9–15] drift-wave,[16–18] and ion-cyclotron[19–26] instabilities. Interestingly, in the case of the shear-modified ion-cyclotron instability, the simultaneous appearance of multiharmonic features are observed in the fluctuation spectrum, in contrast to the spectra of the conventional current-driven electrostatic ion-cyclotron instability which typically has a single dominant spectral feature. However, there is no report that drift waves with multiple harmonics, or high azimuthal mode numbers, can be excited by the parallel-flow-velocity shear.

The aim of the present work is to carry out laboratory experiments on the shear-modified drift-wave instabilities having high mode numbers. The parallel flow shear is controlled using a concentrically segmented plasma source.[27] The observation of high azimuthal mode numbers allows additional insight to be developed regarding the competition between inverse electron Landau damping and shear-modified ion Landau damping.

In Sec. II, the experimental apparatus and methods are described. Experimental results are presented in Sec. III and are discussed in Sec. IV. Conclusions are included in Sec. V.

## II. EXPERIMENTAL APPARATUS

Experiments are performed in the West Virginia University Q machine (WVUQ).[28,29] The schematic of the experimental apparatus is shown in Fig. 1. A collisionless plasma is produced by a modified plasma synthesis method,[27] where barium-ion and electron emitters are oppositely set at cylindrical machine ends under a strong magnetic field of $B=2.88$ kG. The ion emitter is a 7.6-cm-diameter rhenium-coated tungsten (Re-W) hot plate. The hot plate is concentrically segmented into three sections with the outer diameters of 1.8, 4.8, and 7.6 cm, each of which is heated $(T_{ie1}, T_{ie2}, T_{ie3})$ by electron bombardment from outboard filaments and individually biased $(V_{ie1}, V_{ie2}, V_{ie3})$. Typically, $1800\ ^\circ\mathrm{C} \simeq T_{ie1} \geqslant T_{ie2} \gg T_{ie3} \simeq 300\ ^\circ\mathrm{C}$. In addition, the biased electron emitter $(V_{ee})$, an 8-cm-diameter tungsten (W) hot plate, is mounted at a distance of $z=300$ cm from the ion emitter.

A negatively biased grid, the voltage of which is typically $V_g=-40$ V, is installed at a distance of $z=30$ cm from the ion emitter surface. Since the grid reflects the electrons flowing from each emitter, the plasma potential in the measurement region between the grid and the electron emitter is determined by the bias of the electron emitter, and thus, the voltage applied to the ion emitter can control the field-aligned ion flow velocity and its shear.[27] The field-aligned barium-ion flow velocity and the plasma parameters are measured by the laser-induced fluorescence,[28,30,31] an emissive probe, and a small Langmuir probe, respectively.

For $V_{ie1,2,3} > V_{ee}$, we obtain $v_d > 0$, where $v_d > 0$ is associated with $\vec{v}_d$ in the $\vec{B}$ direction and $v_d < 0$ is associated with

[a)]Electronic address: kaneko@ecei.tohoku.ac.jp

 

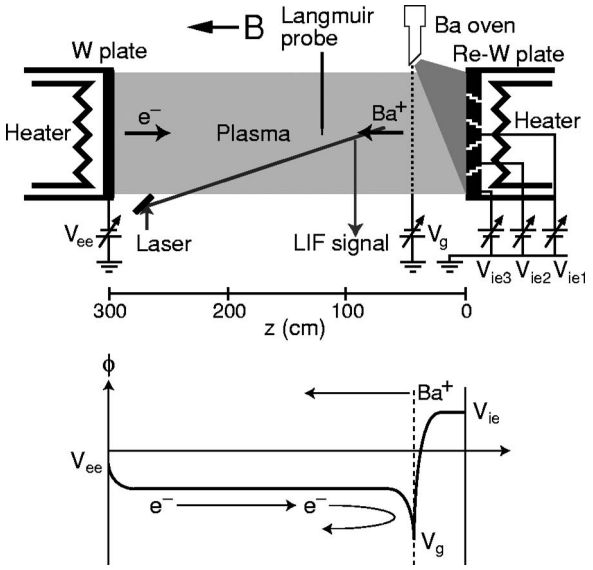


FIG. 1. Schematic of experimental setup of parallel flow velocity shear.

$\vec{v}_d$ in the $-\vec{B}$ direction. For $V_{ie1}>V_{ie2}>V_{ie3}>V_{ee}$, we obtain $dv_d/dr<0$, whereas for $V_{ie3}>V_{ie2}>V_{ie1}>V_{ee}$, we obtain $dv_d/dr>0$, as expected. We model the region near the plasma-column edge using slab geometry, in which case $dv_d/dr=dv_d/dx$ in the limit of the radial position of the drift waves is much larger than both the ion gyroradius and the annular width of the radial profile of fluctuation amplitude. Although the drift waves are excited near the plasma-column edge, where the density gradient is significant, the requirements of this limit are only marginally met here and so precise quantitative agreement between slab-geometry theory and cylindrical-geometry experiment are not expected.

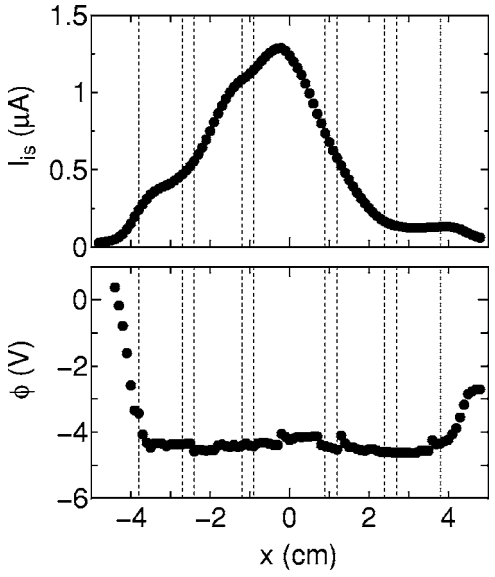


FIG. 2. Radial profiles of ion saturation current $I_{is}$ and floating potential $\phi$ for $V_{ie1}=V_{ie2}=0$ V, $V_{ee}=-2.5$ V, $V_g=-40$ V at $z=120$ cm.

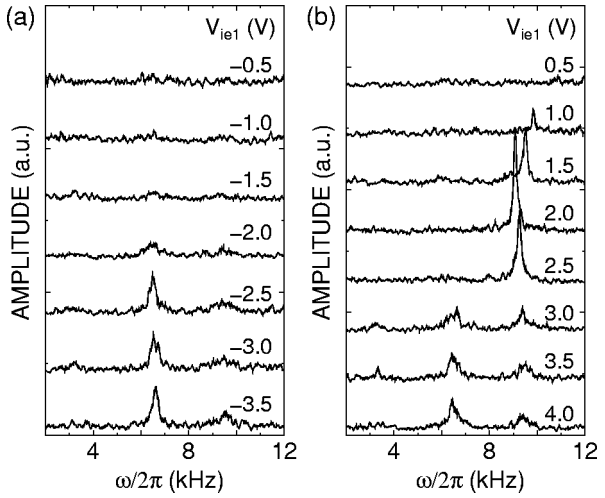


FIG. 3. Frequency spectra of electron saturation current of the probe with $V_{ie1}$ as a parameter for $V_{ie2}=0$ V, $V_{ee}=-2.5$ V, $V_g=-40$ V at $x=-2.5$ cm.

## III. EXPERIMENTAL RESULTS

Figure 2 presents radial profiles of ion saturation current $I_{is}$ of the Langmuir probe and floating potential $\phi$ of the emissive probe for $V_{ie1}=V_{ie2}=0$ V at $z=120$ cm, where the dotted lines in the figure correspond to the boundaries of the segmented ion emitter. In the present experiment, $V_{ie3}$ is always kept at 0 V. The plasma density $n_p$, which is derived from the peak in the ion saturation current profile, is approximately $10^9$ cm$^{-3}$ on the cylindrical axis and gradually decreases toward the plasma-column edge. The plasma potential, which is shifted in voltage insignificantly from the floating potential of the emissive probe $\phi$ ($\simeq -4.5$ V), is radially uniform within the third electrode. This flat region corresponds to the diameter of the electron emitter. As usual in Q-machine plasma under electron-rich conditions, the plasma potential is negative on the cylindrical axis of the plasma column and increases toward the plasma-column edge.

When $V_{ie1}$ and/or $V_{ie2}$ are varied, no appreciable difference of the radial potential profiles is found. This result suggests that the plasma potential is determined by the voltage applied to the electron emitter $V_{ee}$, and we indeed confirm that the plasma potential is controlled by $V_{ee}$. As expected when the ions are accelerated by the difference between the potential of the plasma (i.e., on the electron emitter side of the mesh) and the potential of the ion emitter, the ions have the field-aligned flow energy controlled by the difference between the bias voltages applied to the ion and electron emitters.[27] When $V_{ie1}$ and $V_{ie2}$ are individually varied for the fixed $V_{ee}$, controllable parallel ion flow velocity shear is generated within the cylindrical region that approximately maps magnetically to the boundary between the first and second segments of the ion emitter as presented in Refs. 27 and 28.

In Fig. 3, frequency spectra of fluctuations in the electron saturation current of the Langmuir probe are presented, with $V_{ie1}$ as a parameter, $V_{ie2}=0$ V, $z=120$ cm, and at $x=-2.5$ cm, which corresponds to near the plasma-column edge. Amplitudes of the spectra are measured in linear scale. When $V_{ie1}$ is nearly equal to $V_{ie2}$, the fluctuations are small

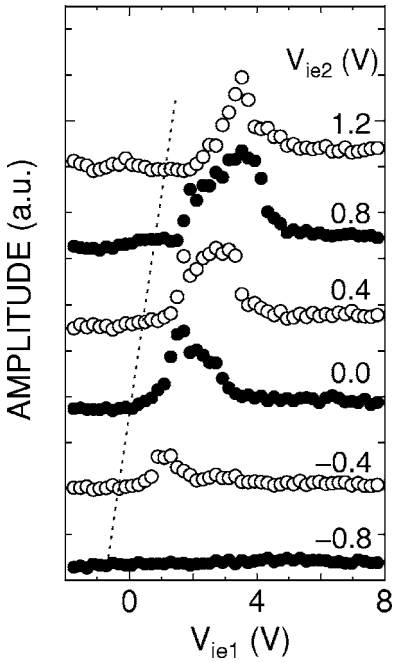


FIG. 4. Fluctuation amplitudes as a function of $V_{ie1}$ and $V_{ie2}$ at $x=-2.5$ cm for $\omega/2\pi \simeq 9.5$ kHz.

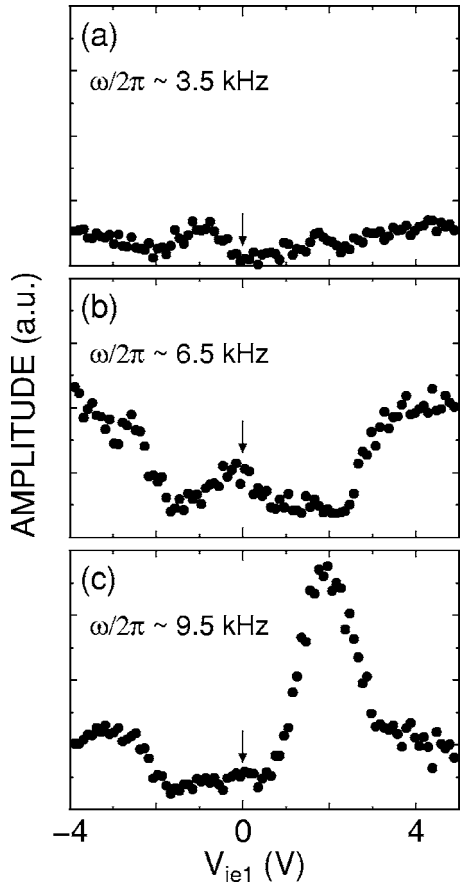


FIG. 5. Fluctuation amplitudes as a function of $V_{ie1}$ for $V_{ie2}=0$ V, $B=2.88$ kG at $x=-2.5$ cm. (a) $\omega/2\pi \simeq 3.5$ kHz, (b) $\omega/2\pi \simeq 6.5$ kHz, and (c) $\omega/2\pi \simeq 9.5$ kHz. Here, the arrows indicate the value of $V_{ie1}$ corresponding to the absence of velocity shear.

and show no clear spectral structure. However, with a decrease [Fig. 3(a)] or an increase [Fig. 3(b)] in $V_{ie1}$, namely, as the magnitude of parallel shear strength increases, the fluctuation amplitude gradually becomes large. For $V_{ie1}>0$, shown in Fig. 3(b), modes with frequencies of $\omega/2\pi=3.5$ kHz, 6.5 kHz, and 9.5 kHz are excited. When $V_{ie1}$ exceeds 0.5 V, the mode with $\omega/2\pi=9.5$ kHz is first excited in the weak shear condition and then grows, reaches maximum amplitude, and eventually becomes smaller as $V_{ie1}$ and shear strength increase further. This demonstrates that exciting the mode with $\omega/2\pi=9.5$ kHz requires nonzero shear. At the large shear condition, the mode with $\omega/2\pi=6.5$ kHz starts to grow at $V_{ie1}\simeq 2.5$ V. Even stronger shear which is generated by even larger $V_{ie1}$ is required to excite the mode with $\omega/2\pi=3.5$ kHz. Here, we will concentrate on the excitation threshold of each mode rather than the value of $V_{ie1}$ associated with the maximum in each mode's amplitude.

For $V_{ie1}<0$, shown in Fig. 3(a), the mode with $\omega/2\pi=6.5$ kHz is observed to grow for $V_{ie1}<-2.0$ V. When $V_{ie1}$ is decreased further, the ions in the central core of the plasma column have difficulty flowing into the measurement region because the potential difference between the electron and the ion emitters $(V_{ee}-V_{ie1})$ becomes insufficiently negative. As a result, the plasma column becomes hollow and the radial density profile includes regions in which the radial density gradient is positive, likely influencing the drift-wave instability in an undesirable way. Thus, we concentrate on the modes excited for $V_{ie1}>0$ in order to isolate the effect of flow velocity shear on the low-frequency instabilities.

Since the 9.5-kHz mode's spectral feature has the maximum value at $\omega/2\pi=9.5$ kHz and has a width that is insensitive to the values of $V_{ie1}$ and $V_{ie2}$ in this experimental condition, we adopt the fluctuation amplitude at $\omega/2\pi=9.5$ kHz as this mode's amplitude for the purpose of documenting in Fig. 4 the effects of changing $V_{ie1}$ and $V_{ie2}$ on the 9.5-kHz mode amplitude. When $V_{ie1}$ is nearly equal to $V_{ie2}$, the zero-shear condition, which is given as a dotted line in Fig. 4, the mode amplitude is negligible as already shown in Fig. 3. Increasing $V_{ie1}$ beyond $V_{ie2}$ causes the mode amplitude to gradually become large and reach a maximum value for $V_{ie1}-V_{ie2}\simeq 2$ V. When $V_{ie1}$ and $V_{ie2}$ are imagined to be varied simultaneously, keeping fixed $V_{ie1}-V_{ie2}\simeq 2$ V, this maximum mode amplitude appears to be relatively insensitive to the bias voltages for $V_{ie2}>0$. This is evidence that the excitation mechanism depends strongly on flow shear and weakly on flow velocity. For $V_{ie2}<0$, the mode amplitude gradually decreases with a decrease in $V_{ie2}$, and reaches the background fluctuation level for $V_{ie2}=-0.8$ V even when $V_{ie1}-V_{ie2}$ is kept 2 V. The results for $V_{ie2}<0$ might be understood if either (1) the maximum density gradient decreases significantly when $V_{ie2}<0$ so that the drift-wave amplitude becomes negligible, (2) the plasma column diameter shrinks when $V_{ie2}<0$ so that the location of the density gradient shifts radially inward, causing the mode to either shift away from the measuring probe or become negligible in amplitude everywhere, or (3) the role of ion flow velocity $v_d$ is important to the drift-wave excitation mechanism when $V_{ie2}<0$.

As a next step, we compare the characteristics of the

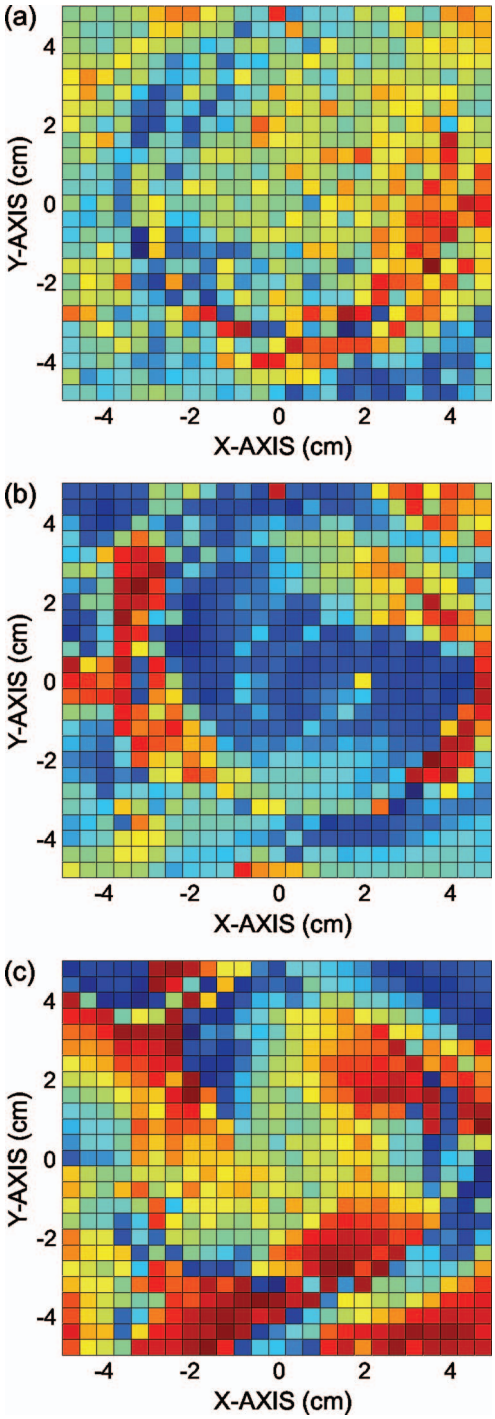


FIG. 6. (Color). Two-dimensional profile of fluctuation phase for (a) $\omega/2\pi \simeq 3.5$ kHz, $V_{ie1}=4$ V (b) $\omega/2\pi \simeq 6.5$ kHz, $V_{ie1}=4$ V, and (c) $\omega/2\pi \simeq 9.5$ kHz, $V_{ie1}=2$ V, where $V_{ie2}=0$ V, $V_{ee}=-2.5$ V, $B=2.88$ kG, and $z=95$ cm.

three modes. Figure 5 shows the fluctuation amplitudes at (a) $\omega/2\pi=3.5$ kHz, (b) $\omega/2\pi=6.5$ kHz, and (c) $\omega/2\pi=9.5$ kHz as a function of $V_{ie1}$ for $V_{ie2}=0$ V at $x=-2.5$ cm, where the arrows indicate the value of $V_{ie1}$ corresponding to the absence of velocity shear. It is found that each mode is excited by a different value of shear strength with lower-frequency modes requiring larger shear strength. When $V_{ie1}$ is increased, the mode with $\omega/2\pi=9.5$ kHz is excited first, at $V_{ie1} \simeq 0.5$ V, and has maximum amplitude at $V_{ie1} \simeq 2$ V.

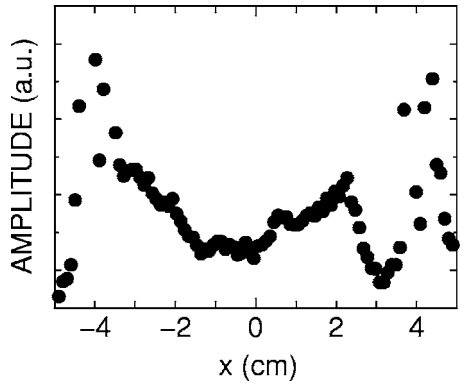


FIG. 7. Radial profile of the fluctuation amplitude for $V_{ie1}=2$ V, $V_{ie2}=0$ V, $\omega/2\pi \simeq 9.5$ kHz, $B=2.88$ kG at $z=120$ cm.

The mode with $\omega/2\pi=6.5$ kHz, on the other hand, is excited second, at $V_{ie1}=2.5$ V, and has maximum amplitude at $V_{ie1}>3.5$ V. The mode with $\omega/2\pi=3.5$ kHz is not almost excited within $V_{ie1}<5$ V, which implies that exciting this mode needs $V_{ie1}>5$ V. The excitation threshold of each mode is discussed in Sec. IV. Note that the 9.5-kHz mode-amplitude maximum appears to be larger than the 6.5-kHz mode-amplitude maximum.

To readily identify the azimuthal component of each mode's wavevector, we measure the two-dimensional $(x,y)$ profile of fluctuation phase in the plasma-column cross section. The data acquisition is performed at 4 mm intervals in the range of $-5$ cm$<x,y<5$ cm, namely, the number of data points is 625 $(=25\times25)$, and the weighted-average technique is used to obtain the data. The phase is measured with reference to a spatially fixed Langmuir probe located at an axial distance of 25 cm from the two-dimensionally translatable probe. Since the size of the probe tip is less than 1 mm in length and 0.5 mm in outer diameter, the insertion of the probe into the plasma does not change the frequency spectrum obtained by the above-mentioned reference probe fixed in the plasma, namely, the probe does not perturb the plasma even in the shear region. Figure 6 presents the phase profiles measured at $z=95$ cm for the modes with (a) $\omega/2\pi=3.5$ kHz, (b) $\omega/2\pi=6.5$ kHz, and (c) $\omega/2\pi=9.5$ kHz. Deep red and violet indicate the phase of $+\pi$ and $-\pi$, respectively, relative to the reference probe. Pale green corresponds to zero relative phase, with pale yellow and pale blue bordering zero on the positive and negative sides of zero, respectively. Concentrating on an imaginary circle at $r=3$ cm, it is found that the fluctuations at 3.5, 6.5, and 9.5 kHz correspond to the azimuthal modes of $m=1$, 2, and 3, respectively.

Figure 7 shows a radial profile of the fluctuation amplitude for $V_{ie1}=2$ V, $V_{ie2}=0$ V, $\omega/2\pi \simeq 9.5$ kHz, $B=2.88$ kG at $z=120$ cm. The fluctuation amplitudes are larger near the plasma-column edge, where the density gradient is relatively large, thus the data in the range 2.5 cm$<|x|<4.0$ cm should receive maximum emphasis. The data in the range $|x|>4$ cm, i.e., beyond the plasma-column edge, should receive negligible emphasis. The value of $k_\theta$ is inferred from the data in Fig. 6 with $k_\theta=m/r$ for either $m=1$, 2, or 3 and $r=3$ cm. Using a radially translatable, rotatable, two-tip, Langmuir

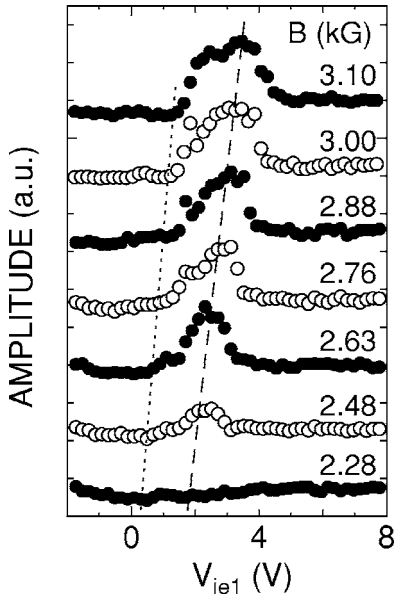


FIG. 8. Fluctuation amplitudes as a function of $V_{ie1}$ for $V_{ie2}=0$ V, $\omega/2\pi \simeq 9.5$ kHz at $x=-2.5$ cm with magnetic field $B$ as a parameter.

probe array with 5-mm probe spacing, $k_z$ is measured to be $(0.2\pm0.1)$ cm$^{-1}$. Since $k_z/k_\theta \simeq 0.2 \ll 1$ and the mode amplitude is larger where the density gradient is large, these fluctuations are identified as the drift-wave instability. In this case, the drift-wave instability is enhanced by the ion flow velocity shear colocated with the density gradient.

Figure 8 shows the fluctuation amplitude of the mode $m=3$ ($\omega/2\pi \simeq 9.5$ kHz) as a function of $V_{ie1}$ with the magnetic field $B$ as a parameter, where $V_{ie2}=0$ V, $V_{ee}=-2.5$ V. When $B$ is increased from 2.28 kG to 3.10 kG, the mode amplitude becomes large. Both the threshold of $V_{ie1}$ at which the mode is excited and the value of $V_{ie1}$ at which the maximum mode amplitude occurs are found to gradually increase with an increase in $B$, as shown with dotted and dashed lines, respectively, to guide the eye in Fig. 8.

## IV. DISCUSSION

The above experimental results are now theoretically analyzed using a slab-geometry kinetic theory that includes the effects of parallel flow velocity $v_d$, its shear $dv_d/dx$, and the azimuthal mode number $m$. Ion-temperature anisotropy, observed in the experiment,[28] is not included. From the dispersion relation, the real frequency $\omega_r$ and the growth rate $\gamma$ of the drift-wave instability for the low-frequency range ($\omega \ll \omega_{ci}$) are given by[16]

$$\omega_r (\equiv \omega_{\rm obs} - k_z v_d) = \frac{\omega_e^*}{2} + \sqrt{\left(\frac{\omega_e^*}{2}\right)^2 + \sigma^2 k_z^2 C_s^2}, \tag{1}$$

$$\frac{\gamma}{\omega_r} = \sqrt{\frac{\pi}{2}} \frac{\omega_r}{\tau(2\omega_r - \omega_e^*)} \frac{\omega_r}{k_z v_{ti}} \left[ \sqrt{\frac{\tau^3}{\mu}} \left( \frac{k_z v_d + \omega_e^*}{\omega_r} - 1 \right) - \sigma^2 \exp\left( -\frac{\omega_r^2}{2(k_z v_{ti})^2} \right) \right], \tag{2}$$

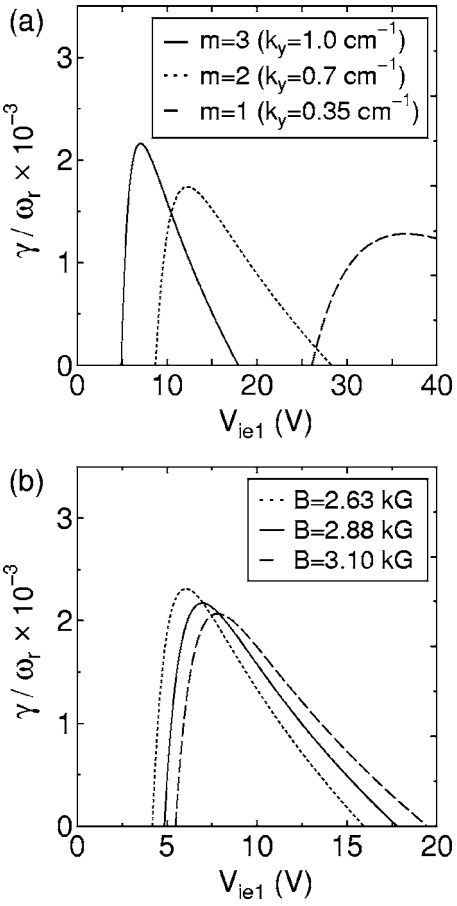


FIG. 9. Predicted dependence of growth rate $\gamma$ of drift-wave instability on $V_{ie1}$, where (a) azimuthal mode number $m$ is varied for $B=2.88$ kG and (b) magnetic field $B$ is varied for $m=3$ ($k_y=1.0$ cm$^{-1}$). For the solid line, the value at $\sigma^2$ ranges from 15 at the leftmost zero crossing to 40 at the rightmost zero crossing.

$$\sigma^2 \equiv 1 - \frac{k_y}{k_z} \frac{1}{\omega_{ci}} \frac{dv_d}{dx}, \tag{3}$$

where $\tau \equiv T_i/T_e$, $\mu \equiv m_i/m_e$, $v_{ti} \equiv (T_i/m_i)^{1/2}$, $C_s \equiv (T_e/m_i)^{1/2}$, $k_y = m/r$ ($r=3$ cm), $\omega_{\rm obs}$ and $\omega_r$ are the real frequency of the drift-wave instability in the laboratory frame and in the ion frame, respectively, and $k_z$ and $k_y$ are the axial and azimuthal components of the mode's wavevector, respectively. We express the effect of the density gradient in terms of the electron diamagnetic drift frequency $\omega_e^*$ ($=k_y T_e \kappa/eB$), where $\kappa = -d \ln n/dx$. The first and second terms in the large brackets of Eq. (2) represent the effects of inverse electron Landau damping and shear-modified ion Landau damping, respectively. The azimuthal mode number and the magnetic field influence the quantity $\sigma^2$ because the expression for $\sigma^2$ contains $k_y$ and $\omega_{ci}$.

The growth rate $\gamma$ is calculated using $k_y=0.35$, 0.7, and 1.0 cm$^{-1}$ for $m=1$, 2, and 3, respectively. Figure 9 shows the calculated growth rate $\gamma$ as a function of $V_{ie1}$ for a fixed $V_{ie2}$ (=0 V). The potential difference between $V_{ie1}$ and $V_{ie2}$ corresponds to the flow-velocity difference, i.e., velocity shear, which is described as

$$\frac{dv_d}{dx} \simeq \sqrt{\frac{2e}{m_i}}\left(\frac{\sqrt{V_{ie2}-\phi}-\sqrt{V_{ie1}-\phi}}{\Delta x}\right), \tag{4}$$

where $\Delta x$ (=3 mm) is the gap width of the segmented ion emitter. The growth rate for $k_y=1.0\ \mathrm{cm}^{-1}$ is larger than those for $k_y=0.35$ and $0.7\ \mathrm{cm}^{-1}$ at $B=2.88$ kG as shown in Fig. 9(a). This is consistent with the experimental observations in Figs. 3 and 5 that the amplitude of the 9.5-kHz mode is larger than the amplitudes of the 3.5-kHz and 6.5-kHz modes, assuming that saturated mode amplitude is approximately proportional to the growth rate. Furthermore, the excitation-threshold value of $V_{ie1}$, for which $\gamma=0$, is found to decrease for increasing values of $k_y$. This can be understood by noticing that the threshold value of $\sigma^2$ for instability can be held constant by increasing $k_y$ as $dv_d/dx$ decreases, for fixed magnetic-field strength. Since the theoretical excitation threshold for $k_y=0.35\ \mathrm{cm}^{-1}$ is much larger than those for $k_y=0.7$ and $1.0\ \mathrm{cm}^{-1}$, exciting the mode with $\omega/2\pi=3.5$ kHz is considered to need larger shear strength compared with the modes with $\omega/2\pi=6.5$ and 9.5 kHz, and as a result, the amplitude of the 3.5-kHz mode is kept small within $V_{ie1}<5$ V as shown in Fig. 5(a). In Fig. 9(b), the growth rate is calculated with the magnetic field $B$ as a parameter for $k_y=1.0\ \mathrm{cm}^{-1}$. The threshold of $V_{ie1}$ increases with an increase in $B$. This can be understood by noticing that the threshold value of $\sigma^2$ for instability can be held constant by decreasing $\omega_{ci}$ as $dv_d/dx$ decreases, for fixed azimuthal mode number.

These calculated results are in good qualitative agreement with the experimental results which are shown in Figs. 5 and 8, suggesting that the observations are explained by the competition between inverse electron Landau damping and shear-modified ion Landau damping.[16] The effects of cylindrical geometry and ion-temperature anisotropy are presently being investigated to arrive at a quantitative comparison between theory and experiment, and will be the subject of a future paper.

## V. CONCLUSIONS

We have carried out basic laboratory experiments on low-frequency instabilities modified by the field-aligned barium-ion flow velocity shear. In the presence of flow shear, drift-wave instabilities with azimuthal mode numbers $m=1$, 2, and 3 are observed simultaneously. The value of the shear strength at which each mode is excited is found to be different, with decreasing mode number requiring increasing shear strength. The value of the shear strength at which the $m=3$ mode is excited is found to depend on magnetic field strength, with increasing magnetic field strength requiring increasing shear strength. These experimental results can be qualitatively explained using a dispersion relation from kinetic theory.

## ACKNOWLEDGMENTS

This work was supported by a Grant-in-Aid for Scientific Research from the Ministry of Education, Culture, Sports, Science and Technology, Japan, and by the National Science Foundation Grant No ATM-0201112, and NASA Grant No. NAG5-10218.

[1] N. D'Angelo, Phys. Fluids **8**, 1748 (1965).
[2] P. J. Catto, M. N. Rosenbluth, and C. S. Liu, Phys. Fluids **16**, 1719 (1973).
[3] S. Migliuolo, J. Geophys. Res. **89**, 27 (1984).
[4] J. F. Drake, A. B. Hassam, P. N. Guzdar, C. S. Liu, and D. McCarthy, Nucl. Fusion **32**, 1657 (1992).
[5] P. K. Shukla, G. T. Birk, and R. Bingham, Geophys. Res. Lett. **22**, 671 (1995).
[6] N. D'Angelo and S. von Goeler, Phys. Fluids **9**, 309 (1966).
[7] T. An, R. L. Merlino, and N. D'Angelo, Phys. Lett. A **214**, 47 (1996).
[8] J. Willig, R. L. Merlino, and N. D'Angelo, J. Geophys. Res. **102**, 27249 (1997).
[9] G. S. Lakhina, J. Geophys. Res. **92**, 12161 (1987).
[10] V. V. Gavrishchaka, S. B. Ganguli, and G. I. Ganguli, Phys. Rev. Lett. **80**, 728 (1998).
[11] G. Ganguli, S. Slinker, V. Gavrishchaka, and W. Scales, Phys. Plasmas **9**, 2321 (2002).
[12] A. Ito and A. Hirose, Phys. Plasmas **11**, 23 (2004).
[13] E. Agrimson, N. D'Angelo, and R. L. Merlino, Phys. Rev. Lett. **86**, 5282 (2001).
[14] C. Teodorescu, E. W. Reynolds, and M. E. Koepke, Phys. Rev. Lett. **88**, 185003 (2002).
[15] C. Teodorescu, M. E. Koepke, and E. W. Reynolds, J. Geophys. Res. **108**, 1049 (2003).
[16] T. Kaneko, H. Tsunoyama, and R. Hatakeyama, Phys. Rev. Lett. **90**, 125001 (2003).
[17] T. Kaneko and R. Hatakeyama, Trans. Fusion Sci. Technol. **47**, 128 (2005).
[18] P. K. Shukla, G. Sorasio, and L. Stenflo, Phys. Rev. E **66**, 067401 (2002).
[19] G. Ganguli, M. J. Keskinen, H. Romero, R. Heelis, T. Moore and C. Pollock, J. Geophys. Res. **99**, 8873 (1994).
[20] P. K. Shukla and L. Stenflo, Plasma Phys. Rep. **25**, 355 (1999).
[21] V. V. Gavrishchaka, G. I. Ganguli, W. A. Scales, S. P. Slinker, C. C. Chaston, J. P. McFadden, R. E. Ergun, and C. W. Carlson, Phys. Rev. Lett. **85**, 4285 (2000).
[22] R. L. Merlino, Phys. Plasmas **9**, 1824 (2002).
[23] E. P. Agrimson, N. D'Angelo, and R. L. Merlino, Phys. Lett. A **293**, 260 (2002).
[24] E. Agrimson, S.-H. Kim, N. D'Angelo, and R. L. Merlino, Phys. Plasmas **10**, 3850 (2003).
[25] C. Teodorescu, E. W. Reynolds, and M. E. Koepke, Phys. Rev. Lett. **89**, 105001 (2002).
[26] M. E. Koepke, C. Teodorescu, E. W. Reynolds, C. C. Chaston, C. W. Carlson, J. P. McFadden, and R. E. Ergun, Phys. Plasmas **10**, 1605 (2003).
[27] T. Kaneko, Y. Odaka, E. Tada, and R. Hatakeyama, Rev. Sci. Instrum. **73**, 4218 (2002).
[28] E. W. Reynolds, T. Kaneko, M. E. Koepke, and R. Hatakeyama, Phys. Plasmas **12**, 072103 (2005).
[29] N. Rynn and N. D'Angelo, Rev. Sci. Instrum. **31**, 1326 (1960).
[30] D. N. Hill, S. Fornaca, and M. G. Wickham, Rev. Sci. Instrum. **54**, 309 (1983).
[31] M. E. Koepke, M. W. Zintl, C. Teodorescu, E. W. Reynolds, G. Wang, and T. N. Good, Phys. Plasmas **9**, 3225 (2002).